ELSEVIER

Engineering Analysis with Boundary Elements 26 (2002) 815–826

ENGINEERING ANALYSIS *with* BOUNDARY ELEMENTS

www.elsevier.com/locate/enganabound

Comparing the conventional displacement BIE and the BIE formulations of the first and second kind in frictionless contact problems

A. Blázquez[a], R. Vodička[b], F. París[c], V. Mantič[c,*]

[a]*Department of Mechanical Engineering, University of La Rioja, Logroño, Spain*
[b]*Faculty of Mechanical Engineering, Technical University of Košice, Košice, Slovakia*
[c]*School of Engineering, University of Seville, Seville, Spain*

Received 27 March 2002; revised 15 July 2002; accepted 19 July 2002

Abstract

There are several formulations of boundary integral equations (BIEs) used in the general numerical procedure known as boundary element method (BEM). There are also several approaches to deal with contact problems using BEM. In this paper, a comparison between the following procedures: the conventional discretization of the displacement BIE by collocations, the Galerkin discretizations of the symmetric BIE formulation of the first kind and the non-symmetric BIE formulation of the second kind, is performed. Although several aspects of these procedures are discussed, the emphasis is put on the accuracy of the results obtained with identical meshes. The comparison is carried out including problems with analytical solutions or in the presence of singularities, covering conforming, advancing and receding contact problems. Linear elements, conforming discretizations of surfaces in contact and absence of friction define the frame where the study is performed.

Keywords: Boundary integral equations; Boundary element method; Symmetric Galerkin BEM; BIE of the second kind; Contact problems

1. Introduction and preliminaries

The application of boundary element method (BEM) to the solution of elastic contact problems is advantageous in comparison to finite element method (FEM), mainly due to the following facts: non-linearities appear only on those boundary parts of the solids that are in contact and the variables appearing in contact conditions are unknowns directly computed by BEM. The aim of this paper is to contribute to the development and understanding of different possibilities that BEM has in approaching contact problems. A numerical comparative study of three basic variants of boundary integral equation (BIE) formulations of the so-called direct BEM applied to the solution of two-dimensional frictionless contact problems is presented in this paper.

Consider an elastic body D with boundary ∂D subjected to an external load. Each point x of the body suffers displacements $\mathbf{u}(x)$. Traction vector $\mathbf{t}(x)$ is obtained by an application of the traction differential operator $\mathbf{T}_x^n$, associated to a unit normal vector $\mathbf{n}(x)$, to the displacements field, $\mathbf{t}(x) = \mathbf{T}_x^n\mathbf{u}(x)$. Columns of the fundamental solution matrix $\mathbf{U}(y,x)$ represent displacement vectors at y originated by the unit point forces applied at x in the directions of the coordinate axes [15]. The following symmetry relations hold for the fundamental solution matrix $\mathbf{U}(y,x) = \mathbf{U}(x,y) = \mathbf{U}^{\mathrm{T}}(y,x)$, where T denotes matrix transposition. Columns of the fundamental tractions matrix evaluated as $\mathbf{T}_y^n\mathbf{U}(y,x)$ represent tractions vectors at y originated by the above-described point forces.

The first BIE formulation studied here is the one traditionally used in BEM applications, defined by the Somigliana displacement identity [17] denoted here as *u*-BIE. For smooth boundary points $x \in \partial D$, the strongly singular *u*-BIE writes as

$$\frac{1}{2}\mathbf{u}(x) + \int_{\partial D} ((\mathbf{T}_y^n\mathbf{U}(y,x))^{\mathrm{T}}\mathbf{u}(y) - \mathbf{U}(y,x)\mathbf{t}(y))\mathrm{d}S_y = 0 \qquad (1)$$

where the integral is evaluated in the Cauchy principal value sense [13,15].

The other two BIE formulations studied here, sometimes called coupled BIE formulations, are obtained by combination of Somigliana displacement and traction identities

* Corresponding author. Tel.: +34-954-487300.
E-mail address: mantic@esi.us.es (V. Mantič).

0955-7997/02/$ - see front matter
PII: S0955-7997(02)00069-3

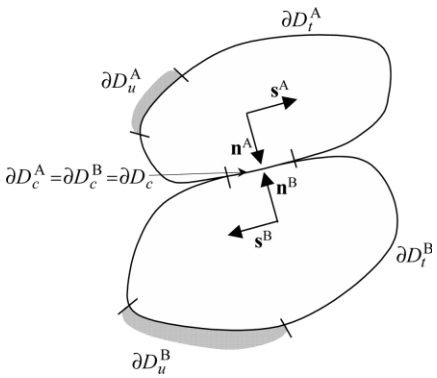

Fig. 1. Contact problem definition.

[5] the latter being denoted here as t-BIE. For smooth boundary points $x \in \partial D$, the hypersingular t-BIE writes as

$$\frac{1}{2}\mathbf{t}(x) + \int_{\partial D} (\mathbf{T}_x^n(\mathbf{T}_y^n \mathbf{U}(y,x))^{\mathrm{T}}\mathbf{u}(y) - \mathbf{T}_x^n \mathbf{U}(y,x)\mathbf{t}(y))\mathrm{d}S_y = 0 \quad (2)$$

where the integral is evaluated in the Hadamard finite part sense [13,15]. The choice of a BIE applied at a point of the boundary depends on the kind of boundary condition prescribed at this point. The symmetric BIE of the first kind [18] is obtained when u-BIE is applied on Dirichlet part (where displacements are prescribed) and t-BIE on Neumann part (where tractions are prescribed) of the boundary, and vice-versa in obtaining the BIE of the second kind [10].

There are some substantial differences between the three BIE formulations above. It should be pointed out that each of these BIE formulations has some advantages over the other two. Some of these advantages are well known, like simplicity of implementation of u-BIE in a BEM code, symmetry of the linear system obtained by a Galerkin discretization of the first kind BIE formulation (this approach is usually called the symmetric Galerkin BEM (SGBEM)), or the lowest condition number of the linear system obtained by a collocation discretization of the second kind BIE formulation. Additionally, some of these advantages have been recently shown in a comparative study of these BIE formulations for two-dimensional Laplace equation [21], such as reliability of results by u-BIE when errors are considered in the maximum and integral L_2 norms, and a relatively low value of error of the results evaluated in the L_2 norm obtained by the SGBEM.

For the solution of contact problems, a BIE formulation has to be coupled with non-linear contact conditions. This can be performed in several ways, a direct imposition of these contact conditions solved by a trial-and-error method, a penalty function and a Lagrange multiplier approaches being the options most frequently used. A direct imposition of contact conditions, originally developed for u-BIE by Andersson et al. [1], and later by París and Garrido [16], is applied for all BIEs studied in the present work.

Contact conditions for the frictionless contact problem analysed here may be grouped into compatibility of normal displacements condition, equilibrium conditions and friction condition

$$\text{Compatibility}: \quad u_n^A + u_n^B = 0 \quad (3)$$

$$\text{Equilibrium}: \quad \mathbf{t}^A - \mathbf{t}^B = 0$$

$$\text{Frictionless}: \quad t_s^A = t_s^B = 0$$

where n denotes the outward normal direction and s the tangential direction to the boundary of each solid in contact, see Fig. 1.

It is noteworthy that in order to maintain an advantageous character of the coupled BIE formulations, namely symmetry and the second kind character of the linear operators associated to the first and second kind BIE formulations, respectively, a special technique of equation assembly is required. Developing previous works by Mantič [12] and Khutoryanskiy [11], respectively, where such assembly techniques were introduced for the first and second kind BIE formulations in solution of multi-zone problems (see also Refs. [8,19]), Vodička [20] has introduced a transformation of contact variables which yields a new assembling technique for solution of frictionless contact problems by coupled BIE formulations. BIEs in these formulations are considered in the local coordinate systems defined by the unit outward normal and tangential vectors ($\mathbf{n}^K$, $\mathbf{s}^K$), $K = A, B$. The new unknown variables at the contact zone, introduced in the above-mentioned assembling technique, are associated to the elastic variables defined in both solids, their physical meaning being (neglecting a multiplicative constant) as follows: $(t_n^A + t_n^B)/2$ represents contact pressure, $u_s^A + u_s^B$ represents relative tangential displacement, and $(u_s^A - u_s^B)/2$ and $(u_n^A - u_n^B)/2$ represent average displacements. Table 1 explains how different BIEs are used in the BEM formulations of the frictionless contact problem studied in the present work.

Note that a different approach to contact problems in the framework of SGBEM was introduced by Eck et al. [7].

It has to be pointed out that the above contact conditions can be imposed either in a strong sense or in a weak sense. The imposition in a strong sense of contact conditions is made in a node-to-node scheme for conforming meshes in contact [16] and in a node-to-point scheme for non-conforming meshes [14]. Imposition in a weak sense developed by Blázquez et al. [2] is working well for both the cases of conforming and non-conforming meshes, no problems having been detected for any of the situations where the use of node-to-point approach produced poor results, see Ref. [3]. It can be proved that for conforming meshes, with a one-to-one correspondence of nodes in both meshes in contact, the strong node-to-node and weak approaches are in fact equivalent.

Selecting two appropriate fields of displacements and applying the virtual work theorem the discretized weak

Table 1
Scheme of applications of equations in BEM formulations of the frictionless contact problem

Boundary part	Equations applied in every BEM formulation		
	Conventional	First kind system	Second kind system
∂D_t^K	u^K-BIE	t^K-BIE	u^K-BIE
∂D_u^K	u^K-BIE	u^K-BIE	t^K-BIE
∂D_c	u^A-BIE	$(u^A\text{-BIE})_n + (u^B\text{-BIE})_n$	$(t^A\text{-BIE})_n + (t^B\text{-BIE})_n$
	u^B-BIE	$(t^A\text{-BIE})_s + (t^B\text{-BIE})_s$	$(u^A\text{-BIE})_s + (u^B\text{-BIE})_s$
	Contact conditions	$(t^A\text{-BIE}) - (t^B\text{-BIE})$	$(u^A\text{-BIE}) - (u^B\text{-BIE})$

compatibility condition takes the expression, see Ref. [2]

$$\sum_k^{\mathrm{NCA}} \int_{\partial D^{kA}} (\mathbf{N}^{kA})^{\mathrm{T}} \mathbf{N}^{kA}\, \mathrm{d}s\, \Delta\mathbf{u}_n^{kA} + \sum_k^{\mathrm{NCA}} \int_{\partial D^{kA}} (\mathbf{N}^{kA})^{\mathrm{T}} \mathbf{N}^{B}\, \mathrm{d}s\, \Delta\mathbf{u}_n^{B} - \sum_k^{\mathrm{NCA}} \int_{\partial D^{kA}} (\mathbf{N}^{kA})^{\mathrm{T}} \mathbf{N}^{kA}\, \mathrm{d}s\, \mathbf{d}_n^{k} = 0 \tag{4}$$

where NCA is the number of elements of body A that belong to the contact zone, $\mathbf{N}^{kA}$ is a matrix that contains the shape functions of the element k of body A, $\mathbf{N}^{B}$ is a matrix that contains the shape functions of all elements of body B that belong to the contact zone, $\Delta\mathbf{u}_n^{kA}$ is a vector that contains the increment of displacements of the nodes of the element k of body A, $\Delta\mathbf{u}_n^{B}$ is a vector that contains the increment of displacements of all nodes of body B that belong to the contact zone, and $\mathbf{d}_n^{k}$ is a vector that contains the normal separation of the nodes of the element k of body A from body B.

Selecting two appropriate fields of tractions and applying the virtual work theorem, the discretized weak equilibrium condition takes the expression

$$\sum_k^{\mathrm{NCB}} \int_{\partial D^{kB}} (\mathbf{N}^{kB})^{\mathrm{T}} \mathbf{N}^{kB}\, \mathrm{d}s\, \Delta\mathbf{t}_i^{kB} - \sum_k^{\mathrm{NCB}} \int_{\partial D^{kB}} (\mathbf{N}^{kB})^{\mathrm{T}} \mathbf{N}^{A}\, \mathrm{d}s\, \Delta\mathbf{t}_i^{A} = 0 \tag{5}$$

where the meaning of the terms is similar to those used in the compatibility equation.

Finally, the frictionless condition is imposed cancelling the tangential stress in all the nodes of body A that belong to the contact zone.

For the purpose of comparison, numerical solutions of three typical contact problems obtained by the above three basic BIE formulations are presented and analysed in the present work. In some of these problems the final contact zone size is unknown. Therefore, because of the non-linear character of the contact conditions, an incremental approach of resolution is required [16]. Due to the fact that the problems analysed correspond to the frictionless cases, an iterative (trial-and-error) approach may be used as well.

In an incremental approach, the increment size is calculated as the amount of load that produces the first change in the contact condition of a node. In an iterative approach the load increment size is fixed, and so changes in the contact conditions of many nodes may occur. A trial-and-error procedure is then needed to generate solutions satisfying equilibrium and compatibility conditions.

BEM codes applied in this study use discretizations by means of continuous linear boundary elements [15]. The comparison between the three BIE formulations is facilitated by using for each problem a unique discretization, with a conforming mesh, i.e. the two surfaces to contact present identical discretizations. Principal features of the BEM codes used are the following: (i) u-BIE approach—collocations of u-BIE at mesh nodes, numerical integrations using eight Gauss points unless otherwise specified, imposition of contact conditions in a weak sense and an incremental procedure of application of load; (ii) coupled BIE formulations approaches—the Galerkin discretization of u-BIE and t-BIE, analytical integrations, a strong imposition of contact conditions and an iterative procedure. A summary of these features is shown in Table 2.

2. Applications

Three classic cases, covering the three conceptually different contact situations, are going to be used as a benchmark to compare the three approaches previously

Table 2
Principal features of the BEM codes

Formulation	Discretization method	Integration	Imposition of contact conditions	Solution approach
u-BIE	Collocations	Numerical	Weak form	Incremental
Coupled BIEs	Galerkin	Analytical	Strong form	Iterative

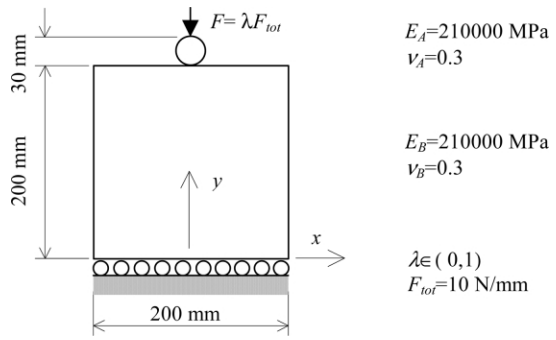

Fig. 2. Advancing contact problem configuration.

mentioned. The first corresponds to the indentation of a cylinder against a foundation, a problem that corresponds to the advancing contact problem solved by Hertz for the case of an infinite foundation. The second problem corresponds to the compression of a thin layer on a foundation, which is a receding contact situation. Finally, the third problem corresponds to the indentation of a punch against a foundation, a conforming contact case involving singularities in the stress field. Plane strain is considered in all the problems studied.

2.1. Indentation of a cylinder against a foundation

The geometry, properties, loads and boundary conditions are defined in Fig. 2. The concentrated load is applied by means of a triangular distribution along the two elements close to the axis y of symmetry. The presence of such an axis permits the symmetry to be applied. The first and second kind BIE formulations use it explicitly (putting elements along the axis of symmetry), whereas in the u-BIE formulation explicit and implicit (not putting elements along the axis of symmetry but integrating along the whole boundary) symmetry are applied, the second case being to all effects comparable, in terms of results, to not considering the presence of symmetry.

The load, as indicated in Fig. 2, is applied by means of a parameter λ, which varies from 0 to 1. The contact algorithms associated to all approaches are able to look for the best solution (length of the contact zone), in accordance with the discretization performed, associated to a value of λ, applying a trial-and-error procedure. The contact algorithm used in u-BIE formulation is additionally prepared to detect the value of λ required to reach the contact at any node of the contact zone discretization performed. The candidate zone to reach contact is modelled with elements of identical length of value 0.00225 mm.

Fig. 3 represents the values of the contact pressure along the contact zone for five different values of λ (0.05, 0.25, 0.5, 0.75, 1.0). As can be observed, the results agree very well with each other and with Hertz solution except, for some cases, at the axis of symmetry and at the extreme of the contact zone. This fact can be clearly appreciated in Fig. 4 where relative contact pressure errors are represented for the particular value of $\lambda = 0.5$, the case where the effect is most attenuated.

At the axis of symmetry the errors that can be considered significant are only associated, as can be more clearly observed in Fig. 5 where only the maximum value of the contact pressure is represented for different values of λ, to the use of explicit symmetry for the u-BIE formulation. An increment in the number of the Gauss points (double the number) to elucidate the reason for these errors did not modify significantly the values found. These errors can be associated to the presence of mixed boundary conditions at the artificial corner originated by the application of the explicit symmetry and are not associated to the contact problem formulation or solution. Nevertheless, it is possible to observe the beneficial effect that the Galerkin formulation (used in first and second kind BIE formulation) has on the

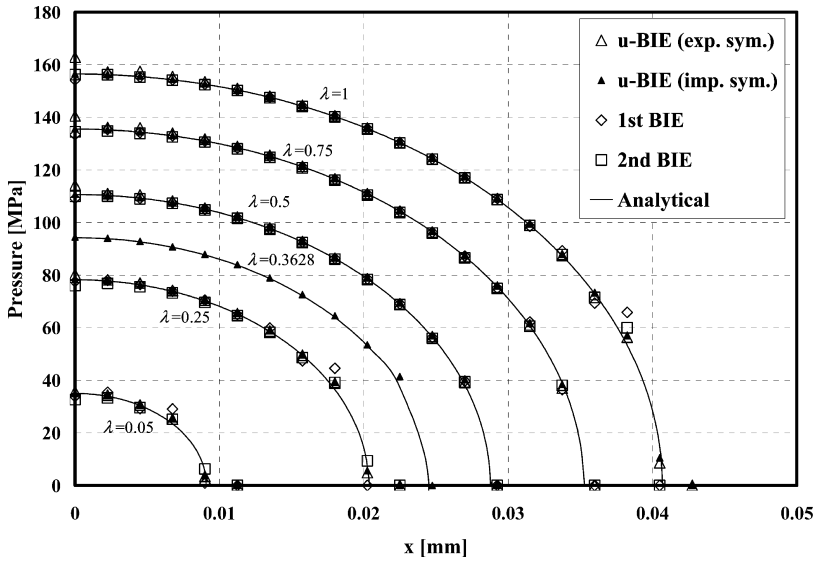

Fig. 3. Contact pressure distribution for different values of λ.

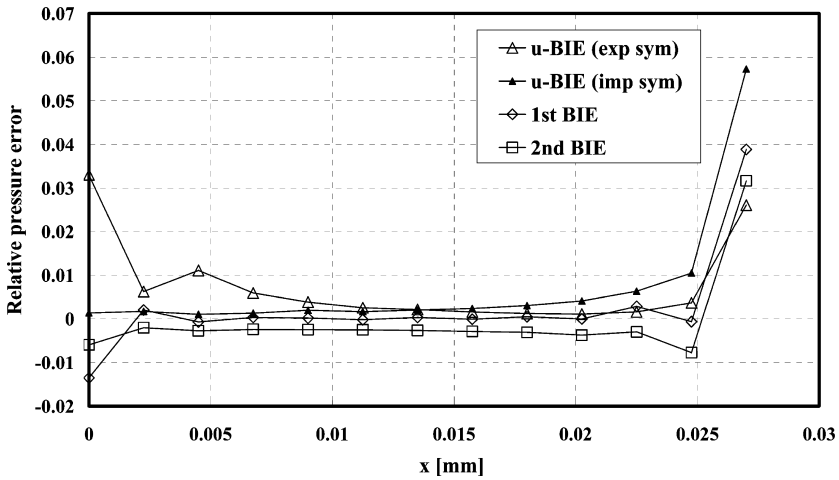

Fig. 4. Relative contact pressure errors for $\lambda = 0.5$.

accuracy at corners with mixed boundary conditions in comparison to the collocation formulation used in *u*-BIE formulation.

With reference to the errors close to the end of the contact zone, clearly noticeable in Figs. 3 and 4, they are of a different nature. First of all, it has to be recognized that the length of the contact zone predicted by the numerical analysis has to be greater than the length predicted by the analytical formula for the same value of the load. This is obvious due to the polygonal nature of the geometry of the boundary in the numerical model, in contrast with the curved geometry of the solid. Thus, the increment of load to produce the contact along a pair of rectilinear elements will always be smaller than in the case of curved surfaces where the contact of the extremes would produce interpenetrations along the elements (Fig. 6), avoidance of these requiring an extra amount of load. (It has in any case to be mentioned that the polygonal nature of the numerical model is only partially taken into account, because only one value of the traction vector is taken at the junctions of the elements, instead of the two ($\mathbf{t}^a$ and $\mathbf{t}^b$ in Fig. 6), strictly speaking singular, values of the traction vector at both sides of the artificial corners, see Ref. [4].)

Once this fact is recognized, the errors for a value of λ that produces the entrance into the contact zone of a certain node (zero value of the contact pressure at the end of the contact zone) ought to be almost negligible. To check the case of one particular value of λ (0.3628) that produces the incorporation of a node into the contact zone, it has been represented (for clarity only for *u*-BIE formulation) in Fig. 3. It can be noticed that in accordance with the former explanation the numerical contact zone is slightly bigger than the analytical contact zone for the load considered. In terms of contact pressure, only a certain error appears at the first node inside the contact zone, having a value slightly higher than the analytical. The reason for this small error is that the linear element used is not able to capture the infinite value of the slope of the stresses at the onset of the contact zone, a very local error compensation appearing

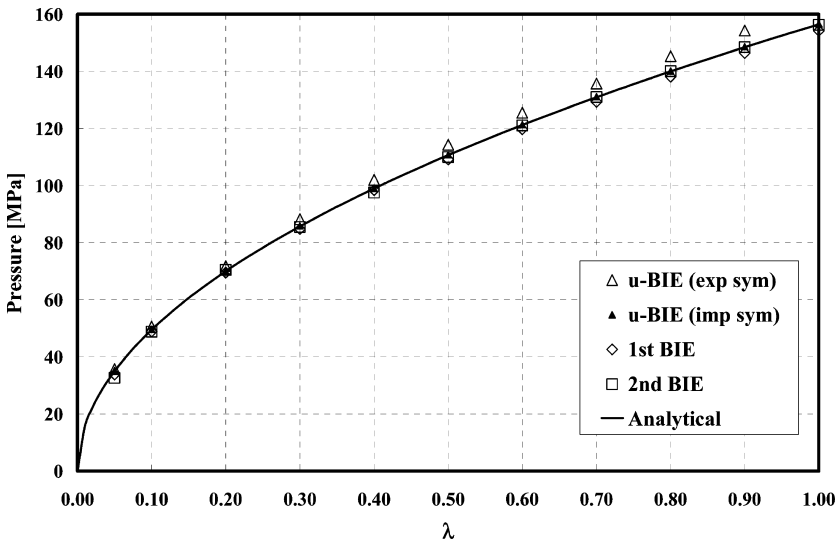

Fig. 5. Contact pressure at the axis of symmetry.

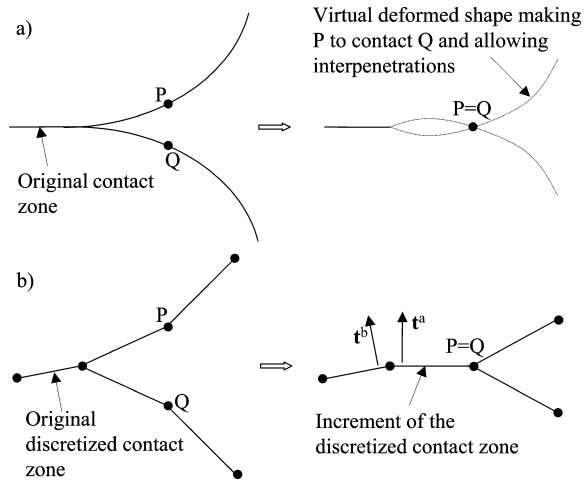

Fig. 6. Contact of: (a) two smooth curved surfaces; (b) two discretized polygonal surfaces.

at the neighbourhood of the end of the contact zone to guarantee the global equilibrium of each solid.

When the value of λ, as is the case for the other values selected and represented in Fig. 3, corresponds to an intermediate value between those corresponding to the incorporation into the contact zone of two consecutive nodes, the contact pressure at the final node of the contact zone is not zero. In Fig. 3, the position of the following node not still in contact, and consequently with zero value of the contact pressure, has also been represented due to the fact that along the element defined by these two nodes there is a linear distribution of load due to the approximation performed, although the element is not strictly in contact. The correct value of the contact zone would be somewhere in the middle of this element. It can again be observed that the errors associated to the lack of accuracy of the discretization performed for the particular value of λ considered (see for instance $\lambda = 1$) are balanced, with respect to the analytical solution, very locally, involving the first node (the first two at most) closest to the end of the contact zone. A detailed view of such a local balance of positive and negative errors of discretized pressures at the end of the contact zone for two particular values of λ, when two consecutive nodes (numbers 14 and 15 in particular) are incorporated into the contact zone, and also for an intermediate value of λ, is plotted in Fig. 7.

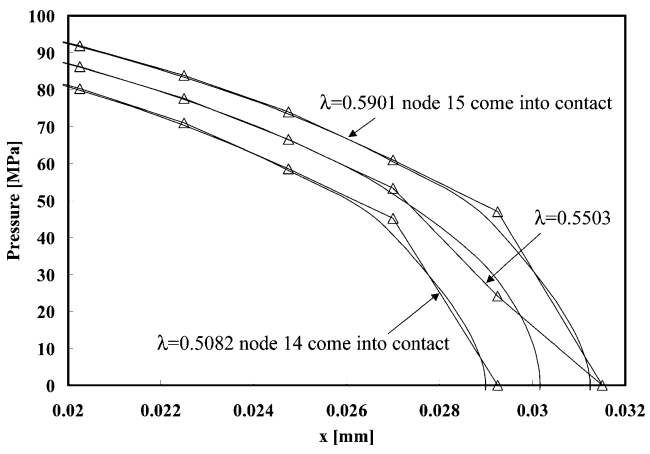

Fig. 7. Local view of pressure distributions at the end of contact zone.

To quantify in any case these errors for values of λ associated to the incorporation of two consecutive nodes into the contact zone, Fig. 8 represents the relative errors of the contact pressure at the last node of the contact zone (node number 14) for intermediate values of λ. Due to the fact, clarified above, that the values of λ in the numerical and analytical models are not coincident for a particular point to reach the contact, relative increments of λ (associated to the numerical or analytical solution) between the contact of the two consecutive nodes (the difference now between numerical and analytical predictions is minimum) are taken in the representation. It can be verified that the error in the contact pressure has a local maximum at an intermediate value of λ and that it achieves a relatively small value when the next node (number 15) is incorporated into the contact zone.

All previously stated for the length of the contact zone can be appreciated in Fig. 9 where the length of the contact zone is represented versus λ.

u-BIE predictions for the values of λ that produce the incorporation of a new node into the contact zone present the small differences previously mentioned, whereas a prefixed value of λ may lead to certain differences of predictions depending on the discretization performed, as has been noticed by means of the results shown in Fig. 8.

2.2. Compression of a thin layer on a foundation

The geometry, properties, loads and boundary conditions are defined in Fig. 10. The concentrated load is applied in a similar manner to the previous problem. All results shown correspond to considering implicit symmetry.

The nature of the problem leads to a final length of the contact zone smaller than the original but independent of the amount of load applied, that indicated in Fig. 10 being then applied in one increment. The length of the contact zone is controlled by the value of the first Dundurs parameter α [9] whose expression is

$$\alpha = \frac{G_2(1-\nu_1) - G_1(1-\nu_2)}{G_2(1-\nu_1) + G_1(1-\nu_2)} \tag{6}$$

where G_1 and ν_1 are, respectively, the shear modulus and Poisson ratio of the layer and G_2, and ν_2 the corresponding values of the foundation.

Fig. 11(a)–(c) represents, respectively, the distributions of the contact pressures along the contact zone with the three procedures for three values of α (0.4, 0 and -0.4). The maximum values of the contact pressure for all the interval of possible values of α (between 1 and -1) are represented in Fig. 12.

The evolution of the size of the contact zone with the variation of the relative stiffness of layer and foundation can

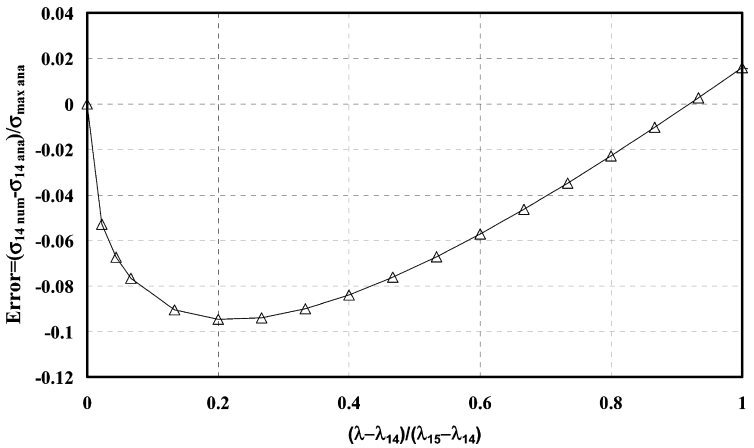

Fig. 8. Relative errors in the contact pressure at the end of the contact zone for values of λ that produce the contact between two consecutive nodes.

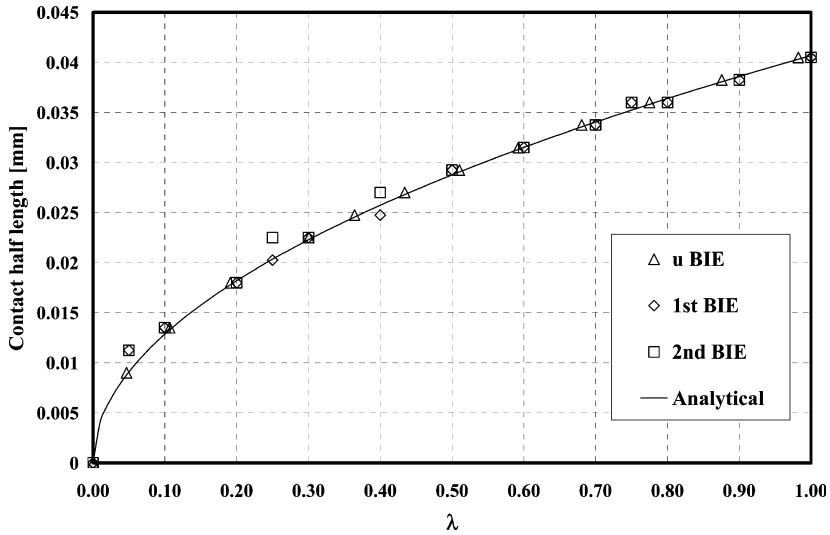

Fig. 9. Half length of the contact zone.

be observed in Fig. 13. The analytical solution of Keer et al. [9] for the case of infinite domains is also represented in the figure.

The results presented in the last three Figures require some additional explanations. Fig. 11(c) only includes results corresponding to u-BIE and the first kind BIE formulations because the second kind BIE formulation leads for $\alpha < 0$ to significantly non-accurate results. It can be observed in Figs. 11 and 13 that in all the range of α, with the exception of $\alpha \leq -0.8$, the length of the contact zone predicted by u-BIE is smaller than the length predicted by the first and second kind BIE formulations, which in turn are very close to each other for $\alpha \geq 0$. This fact leads coherently to finding higher values of the maximum contact pressure with u-BIE in Figs. 11 and 12.

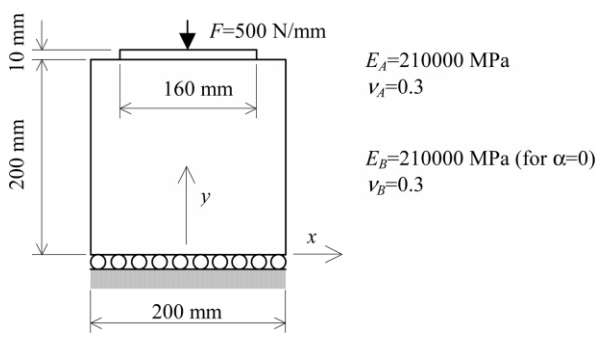

Fig. 10. Receding contact problem configuration.

It can be observed that in the range of positive values of α, the predictions of the three numerical approaches coincide with each other and with Keer et al. solution. In contrast, for negative values of α (the layer is stiffer than the foundation), some differences in the numerical predictions appear, these not always being close to Keer et al. solution. It could be thought that these discrepancies might be due to the different adaptation of the mesh (common for coherence to all cases independently of the value of α) to the nature of the problem. Thus, for $\alpha > 0$ the contact zone is very small and the mesh, prepared to capture the contact zone in this case, was refined only at the end of the expected contact zone. A new mesh with elements of constant length along

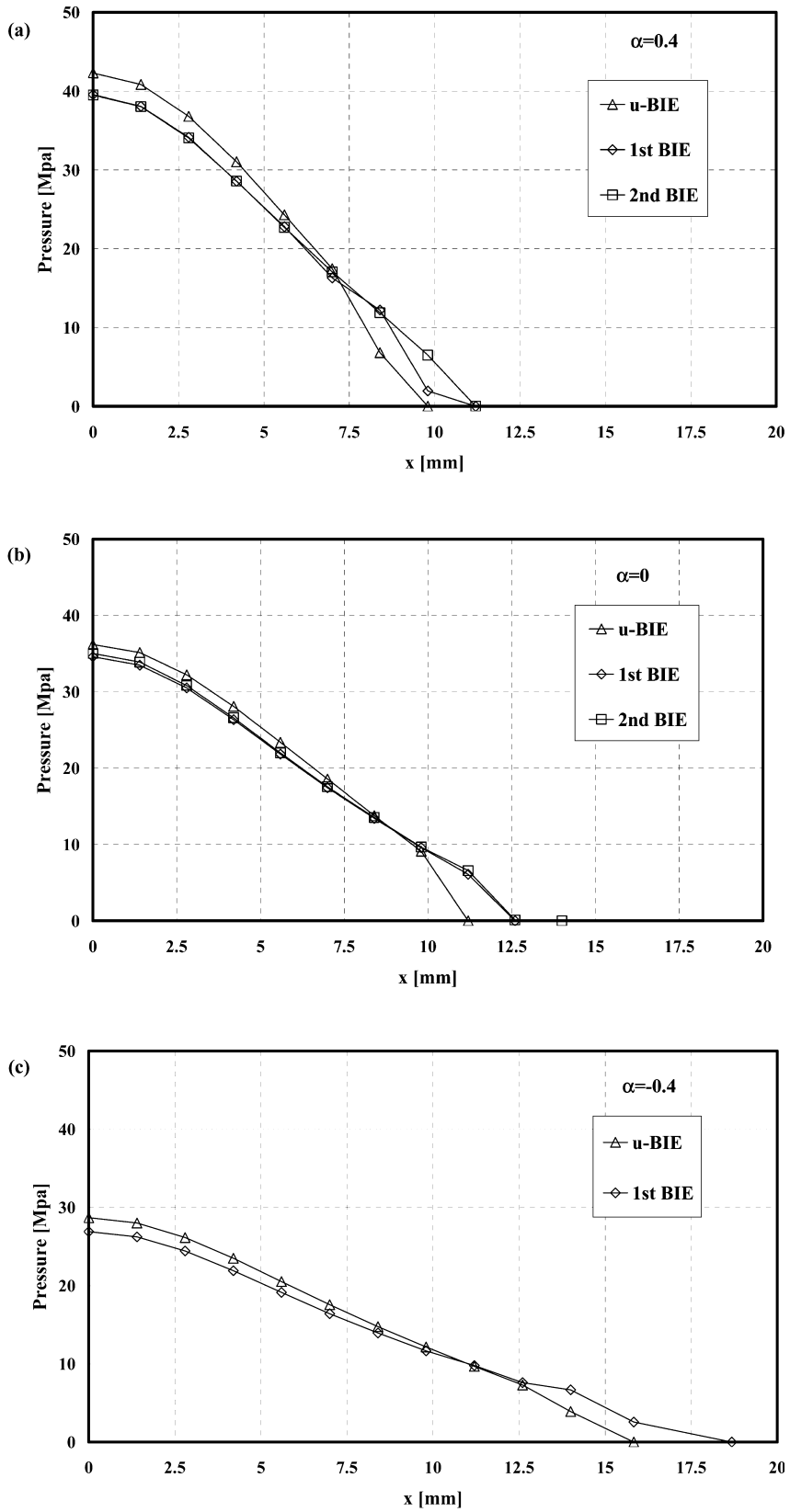

Fig. 11. Contact pressure distribution for different values of Dundurs parameter: (a) $\alpha = 0.4$; (b) $\alpha = 0.0$; (c) $\alpha = -0.4$.

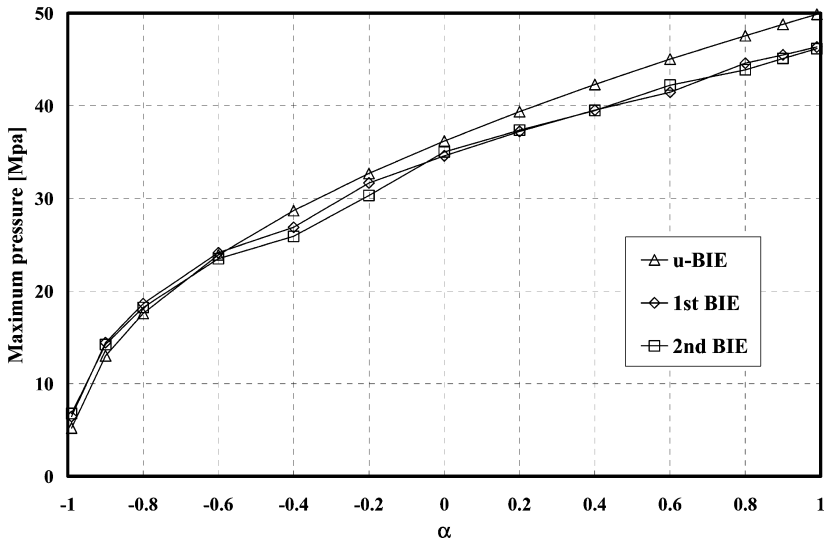

Fig. 12. Contact pressure at the axis of the symmetry.

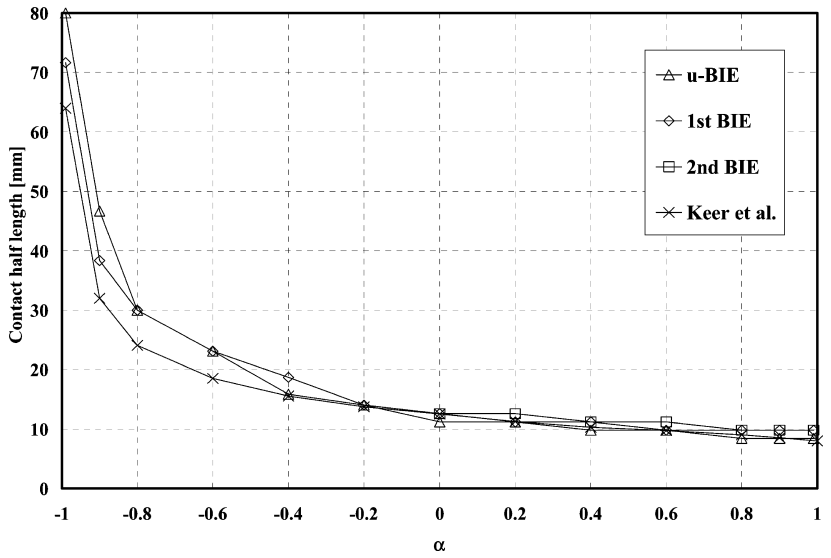

Fig. 13. Half length of the contact zone.

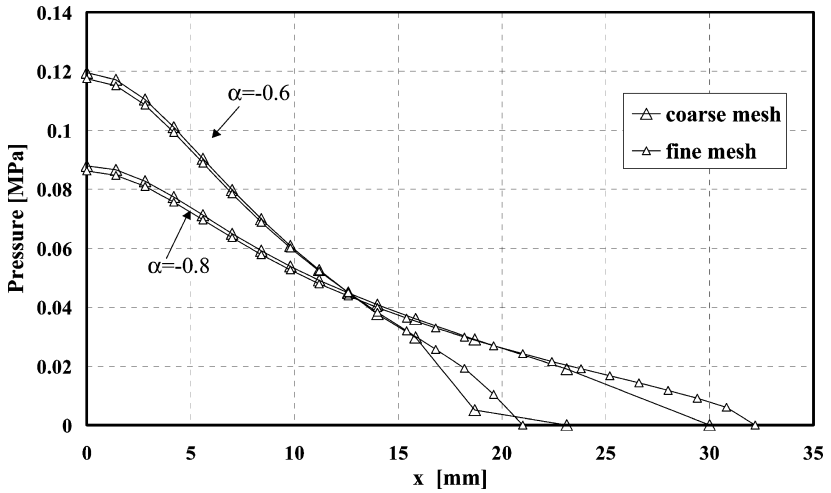

Fig. 14. Contact pressure distribution for negative values of Dundurs parameter, $\alpha = -0.6, -0.8$, obtained by *u*-BIE using the original coarse and a fine mesh.

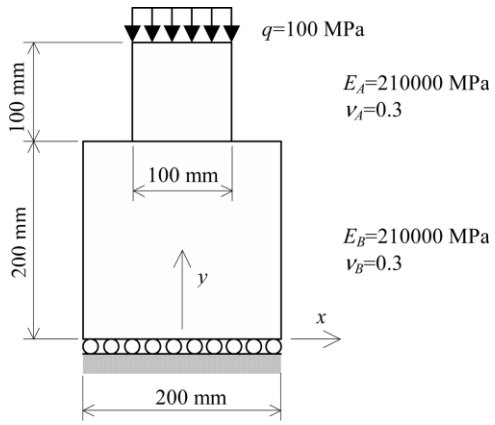

Fig. 15. Conforming contact problem configuration.

the bottom side of the layer was generated, the results being represented in Fig. 14 for the purpose of transparency for *u*-BIE formulation only.

It can be seen that although the solution with this mesh has slightly improved at the end of the contact zone, capturing the solution in a more smooth way, it does not alter significantly the former numerical solution. Arriving at this point, it has to be noted that the numerical solution obtained for the problem modelled is correct and that the discrepancies with respect to the analytical solution are in fact due to the different nature of the problems solved analytical and numerically when α tends to -1. Thus, when α is positive, the length of the contact zone (small) is not affected by the length of the layer. However, when α is negative the length of the contact zone is affected by the length of the layer, infinite in the case solved analytically and finite in the case solved numerically.

2.3. Indentation of a punch against a foundation

The geometry, properties, loads and boundary conditions are defined in Fig. 15. All results shown correspond to considering explicit symmetry.

The nature of the problem leads to a length of the contact zone independent of the amount of load applied and coincident with the original contact zone. The distribution of pressures along the contact zone is represented in Fig. 16, where a detail close to the corner is represented to observe more clearly the effects on the results of the presence of a singularity in the stresses.

It can immediately be noticed that the results are almost indistinguishable in the three approaches along the whole contact zone out of the area dominated by the singularity, where *u*-BIE is the most sensitive approach whereas the first and second kind BIE formulations smooth out in some way the perturbations in the results originated by the singularity.

It is appropriate to evaluate how the three approaches estimate the representative parameters of the stress singular field. To this end, the following general expression for the stresses and particularly for the contact pressure at the neighbourhood of the corner is assumed

$$\sigma \cong \frac{K}{(2\pi r)^{\lambda}} \tag{7}$$

where σ is the contact pressure at a point placed at a distance r from the corner, λ is the order of the singularity and K is the generalized stress intensity factor. The local solution at the neighbourhood of the corner is known [6] presenting a value of $\lambda = 0.2260$.

Considering that the former expression in Eq. (7) can be written in the form

$$\log K \cong \log \sigma + \lambda \log(2\pi r) \tag{8}$$

Fig. 17 represents the estimated values of $\log K$ evaluated by means of the second member of Eq. (8), taking for λ the theoretical value previously mentioned.

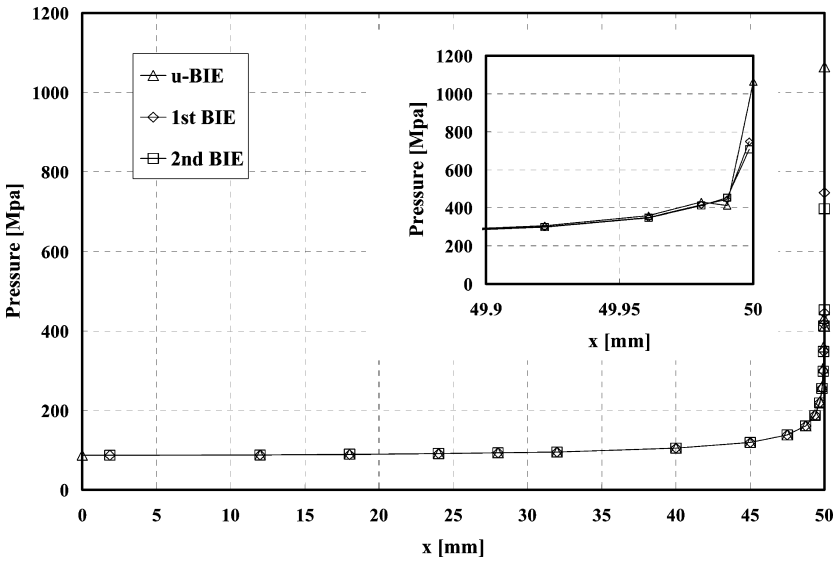

Fig. 16. Singular contact pressure distribution.

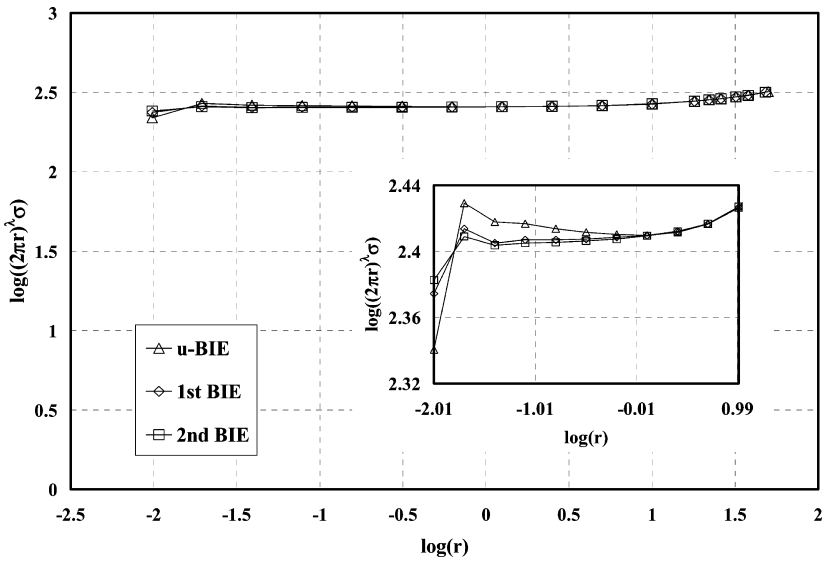

Fig. 17. Estimated value of the logarithm of the generalized stress intensity factor.

To help in quantifying the results shown in Fig. 17, Table 3 shows the results obtained for K (and also those predicted for λ, in order to compare with the analytical value) by means of a least square approach, with points placed at three intervals of values of r. R^2 denotes the correlation coefficient.

Although the results are in all cases quite accurate in evaluating λ, it can be seen again that the first and second kind BIE formulations are better equipped to deal with the presence of singularities. u-BIE would require a finer discretization for the case analysed.

3. Conclusions

The accuracy of numerical solutions of frictionless contact problems obtained by the symmetric BIE formulation of the first kind (SGBEM) and the BIE formulation of the second kind has been compared with the solution obtained using the conventional u-BIE formulation.

The conclusions listed below are based on the solution of three problems associated to the three classic contact situations: advancing contact (indentation of a cylinder), receding contact (compression of a thin layer on a foundation) and conforming contact (indentation of a punch against a foundation). Some features associated to each case are first considered, concluding with a general view of the three procedures considered.

The case of the indentation of a cylinder against a foundation, as representative of the advancing class of contact problems, has been analysed in depth in order to explain the differences found in the estimation of the contact zone in comparison with the one evaluated analytically using Hertz solution. In this respect, it has been shown that in the solution of advancing contact problems it is more appropriate to apply an incremental scheme rather than an iterative one. Thus, the incremental approach allows the load to adapt to a certain extension of the contact zone, whereas the opposite cannot be done in an iterative procedure due to the discontinuous nature of the possible contact zones, in accordance with the discretization performed. The accurate evaluation of size of the contact zone affects the accuracy of the contact pressure at nodes near the end of the contact zone, the lower errors appearing

Table 3
Singularity exponent and generalized stress intensity factor evaluation

		u-BIE	First kind BIE	Second kind BIE
$-2 \le \log r \le 0.1$	λ (error)	0.2115 (-6.9%)	0.2170 (-4.1%)	0.2186 (-3.4%)
	K	173.66	170.69	169.96
	R^2	0.974696	0.995854	0.998243
$-1.75 \le \log r \le 0.1$	λ (error)	0.2354 (4%)	0.2266 (0.27%)	0.2248 (-0.52%)
	K	168.91	168.80	168.73
	R^2	0.999637	0.999661	0.999828
$-1.4 \le \log r \le 0.1$	λ (error)	0.2320 (2.6%)	0.2234 (-1.2%)	0.2226 (-1.5%)
	K	169.44	169.30	169.08
	R^2	0.999972	0.999989	0.999989

at load values corresponding to the incorporation of a new node to the discretized contact zone.

With reference to the problem of indentation of a thin layer against a foundation, it has been found that for a non-negative Dundurs bi-material parameter α all BIE formulations provide similar results, which agree with analytical predictions. Nevertheless, significant differences appear for negative values of α between numerical and analytical solutions. It has been verified, using a refined mesh, that these differences arise due to the differences in the geometry in the problem solved numerically (finite dimensions of the layer and foundation) and in that solved analytically (an infinite layer on an infinite foundation). As could be expected these differences increase with growing contact zone length when α approaches its lower limit value -1.

In order to compare numerical solutions of the indentation of a punch against a foundation, parameters defining the singular behaviour of the contact pressure have been evaluated obtaining results that fit the analytical predictions well. *u*-BIE formulation seems to be more sensitive to the singular nature of the stress state that typically appears in conforming contact problems.

In short, the study carried out has shown that solution by the first and second kind BIE formulations discretized by the Galerkin approach provides a similar degree of accuracy to that obtained by solution of such problems using conventional collocation discretization of *u*-BIE. In fact, in configurations with corners or stress singularities, these novel approaches seem to be less sensitive to the presence of these singularities. The only problem found is in solving problems involving thin solids with relatively high stiffness when applying the second kind BIE formulation. The solution can be unstable and acceptable results can be obtained only for very fine meshes. The reasons for the appearance of this spurious behaviour ought to be clarified in the near future in order to have confidence in the application of this scheme.

Acknowledgements

This work has been supported by the Spanish Dirección General de Enseñanza Superior e Investigación Científica (Project PB98-1118) and by the Scientific Grant Agency of the Slovak Republic (Research Grant 1/8033/01).

References

[1] Andersson T, Fredriksson B, Allan-Persson BG. The boundary element method applied to two-dimensional contact problems. In: Brebbia CA, editor. New developments in boundary elements methods. Southampton: CML Publications; 1980. p. 247–63.

[2] Blázquez A, París F, Mantič V. BEM solution of two-dimensional contact problems by weak application of contact conditions with non-conforming discretizations. Int J Solids Struct 1998;35:3259–78.

[3] Blázquez A, París F, Cañas J. Interpretation of the problems found in applying contact conditions in node-to-point schemes with boundary element non-conforming discretizations. Engng Anal Boundary Elem 1998;21:361–75.

[4] del Caño JC, París F. On stress singularities induced by the discretization in curved contact problems. A BEM analysis. Int J Numer Meth Engng 1997;40:2301–20.

[5] Cruse TA, VanBuren W. Three-dimensional elastic stress analysis of a fracture specimen with an edge crack. Int J Fract Mech 1971;7: 1–15.

[6] Dundurs J, Lee MS. Stress concentration at a sharp edge in contact problems. J Elast 1972;2:109–12.

[7] Eck C, Steinbach O, Wendland WL. A symmetric boundary element method for contact problems with friction. Math Comput Simul 1999; 50:43–61.

[8] Gray LJ, Paulino GH. Symmetric Galerkin boundary integral formulation for interface and multi-zone problems. Int J Numer Meth Engng 1997;40:3085–101.

[9] Keer LM, Dundurs J, Tsai KC. Problems involving a receding contact between a layer and a half space. J Appl Mech 1972;39:1115–20.

[10] Khutoryanskiy NM. Boundary integral and integro-differential equations of the second kind for a mixed boundary value problem of the theory of elasticity (in Russian). Applied problems of strength and plasticity, statics and dynamics of deformable systems. 1981; p. 3–13.

[11] Khutoryanskiy NM. Boundary-contact integro-differential equations of the theory of elasticity for piecewise homogeneous solids (in Russian). Applied problems of strength and plasticity, solution methods of problems of elasticity and plasticity 1981; p. 11–8.

[12] Mantič V. Computational implementation of boundary element method with multilevel substructuring (in Slovak). PhD thesis. Technical University of Košice; 1992.

[13] Mantič V, París F. Existence and evaluation of the two free terms in the hypersingular boundary integral equation of potential theory. Engng Anal Boundary Elem 1995;16:253–60.

[14] París F, Blázquez A, Cañas J. Contact problems with non-conforming discretizations using boundary element method. Comput Struct 1995; 57:829–39.

[15] París F, Cañas J. Boundary element method, fundamentals and applications. Oxford: Oxford University Press; 1997.

[16] París F, Garrido JA. An incremental procedure for friction contact problems. Engng Anal Boundary Elem 1989;6:202–13.

[17] Rizzo FJ. An integral equation approach to boundary value problems of classical elastostatics. Quart Appl Math 1967;25:83–95.

[18] Sirtori S. General stress analysis method by means of integral equations and boundary elements. Meccanica 1979;14:210–8.

[19] Ugodchikoff AG, Khutoryanskiy NM. Boundary element method in the mechanics of a deformable solid body (in Russian). Kazan: University of Kazan Publishing; 1986.

[20] Vodička R. Coupled formulations of boundary integral equations for solving contact problems of elasticity. Engng Anal Boundary Elem 2000;24:407–26.

[21] Vodička R, Mantič V. A comparative study of three systems of boundary integral equations in the potential theory. In: Burczynski T, editor. IUTAM/IACM/IABEM symposium on advanced mathematical and computational mechanics aspects of the boundary element method. Dordrecht: Kluwer Academic Publishers; 2001. p. 377–93.